



Torsion Tool: An automated tool for personalising femoral and tibial geometries in OpenSim musculoskeletal models

Kirsten Veerkamp^{a,b,c,*}, Hans Kainz^d, Bryce A. Killen^e, Hulda Jónasdóttir^{a,f},
Marjolein M. van der Krogt^a

^a Amsterdam UMC, Vrije Universiteit Amsterdam, Department of Rehabilitation Medicine, Amsterdam Movement Sciences, de Boelelaan 1117, Amsterdam, the Netherlands

^b School of Allied Health Sciences, Griffith University, Gold Coast, Australia

^c Griffith Centre for Biomedical & Rehabilitation Engineering (GCORE), Menzies Health Institute Queensland, and Advanced Design and Prototyping Technologies Institute (ADAPT), Griffith University Gold Coast, Australia

^d Centre for Sport Science and University Sports, Department of Biomechanics, Kinesiology and Computer Science in Sport, University of Vienna, Vienna, Austria

^e Human Movement Biomechanics Research Group, Department of Movement Sciences, KU Leuven, Leuven, Belgium

^f Department of Biomechanical Engineering, Faculty of Mechanical, Maritime and Materials Engineering (3mE), Delft University of Technology, Delft, the Netherlands

ARTICLE INFO

Keywords:

Musculoskeletal modeling
Femoral anteversion
Tibial torsion
Cerebral palsy
Subject-specific

ABSTRACT

Common practice in musculoskeletal modelling is to use scaled musculoskeletal models based on a healthy adult, but this does not consider subject-specific geometry, such as tibial torsion and femoral neck-shaft and anteversion angles (NSA and AVA). The aims of this study were to (1) develop an automated tool for creating OpenSim models with subject-specific tibial torsion and femoral NSA and AVA, (2) evaluate the femoral component, and (3) release the tool open-source.

The Torsion Tool (<https://simtk.org/projects/torsiontool>) is a MATLAB-based tool that requires an individual's tibial torsion, NSA and AVA estimates as input and rotates corresponding bones and associated muscle points of a generic musculoskeletal model. Performance of the Torsion Tool was evaluated comparing femur bones as personalised with the Torsion Tool and scaled generic femurs with manually segmented bones as golden standard for six typically developing children and thirteen children with cerebral palsy.

The tool generated femur geometries closer to the segmentations, with lower maximum (−19%) and root mean square (−18%) errors and higher Jaccard indices (+9%) compared to generic femurs. Furthermore, the tool resulted in larger improvements for participants with higher NSA and AVA deviations.

The Torsion Tool allows an automatic, fast, and user-friendly way of personalising femoral and tibial geometry in an OpenSim musculoskeletal model. Personalisation is expected to be particularly relevant in pathological populations, as will be further investigated by evaluating the effects on simulation outcomes.

1. Introduction

Musculoskeletal modelling can be used to evaluate musculoskeletal function in both healthy and pathological populations (e.g., Davico et al., 2020; Fox et al., 2018; Kainz et al., 2019; Steele et al., 2012; van der Krogt et al., 2012; Veerkamp et al., 2019; Wesseling et al., 2016). Often, musculoskeletal models based on a healthy adult are used and scaled to the dimensions of the subject. However, this does not consider subject-specific geometry, such as tibial torsion and femoral neck-shaft angle (NSA) and anteversion angle (AVA), which have been shown to

be aberrant in clinical populations like cerebral palsy (CP; Bobroff et al., 1999; Hicks et al., 2007; Robin et al., 2008). Musculoskeletal models including personalised geometry can be created from magnetic resonance imaging (MRI; Kainz et al., 2016; Killen et al., 2020; Modenese et al., 2018; Scheys et al., 2008; Valente et al., 2017), but are both time and cost intensive and often require a high level of technical skills.

A faster and simpler way to include personalised geometry in musculoskeletal models is by implementing subject-specific torsion angles only (Arnold et al., 2001; Arnold and Delp, 2001; Hicks et al., 2007). However, to date there is no open-source tool available to include this in

* Corresponding author at: Amsterdam UMC, Vrije Universiteit Amsterdam, Department of Rehabilitation Medicine, Amsterdam Movement Sciences, de Boelelaan 1117, Amsterdam, the Netherlands.

E-mail address: k.veerkamp@amsterdamumc.nl (K. Veerkamp).

<https://doi.org/10.1016/j.jbiomech.2021.110589>

Accepted 20 June 2021

Available online 26 June 2021

0021-9290/© 2021 The Author(s). Published by Elsevier Ltd. This is an open access article under the CC BY license (<http://creativecommons.org/licenses/by/4.0/>).

OpenSim (Delp et al., 1990) models. Therefore, we aimed to (1) develop an automated tool for creating an OpenSim model containing subject-specific tibial torsion and femoral NSA and AVA, (2) evaluate this tool for the femur, and (3) make this Torsion Tool openly available.

2. Methodology

2.1. Description of the tool

The Torsion Tool (<https://simtk.org/projects/torsiontool>) was developed in MATLAB (2016a; MathWorks Inc., MA) to personalise geometry that is part of a generic OpenSim model (gait2392; Delp et al., 1990). The tool works for both OpenSim 3.3 and 4.0. Within the tool, subject-specific tibial torsion is achieved by following the methods of Hicks et al. (2007). To implement subject-specific tibial torsion angles, the tibia (as read from the VTP files of the OpenSim model) was divided in three segments along its long axis. The distal third of the tibia and the foot (talus, calcaneus, and toes) were rotated by the entire torsional angle. The joint centres and rotational axes of the ankle, subtalar, and metatarsophalangeal joint were also rotated. The middle third of the tibia was rotated with a linear increasing angle, and the proximal third of the tibia remained unchanged. Torsion angle of the generic tibia was zero degrees.

Subject-specific femoral NSA and AVA angles were implemented using methods of Arnold and Delp (2001) and Arnold et al. (2001), which were extended to also include NSA. Following these methods, it was assumed that these torsions are primarily present in the proximal regions of the femur (Lundy et al., 1998; Robin et al., 2008). The implementation of subject-specific NSA and AVA was modelled as a rotation of the femoral head, neck and proximal shaft of the generic femur. The rotation axes to calculate the NSA and AVA of the generic femur and to apply the subject-specific torsions were based on previous methods (Kainz et al. 2020; Fig. 1). The neck axis was defined to pass

through the centre of the femoral head and the centre of the neck. The shaft axis was defined as the line between the saddle point of the femoral neck and the saddle point between the two epicondyles. The NSA was defined as the angle between the neck axis and shaft axis. The AVA was the angle between the neck axis and the medial-lateral axis through the epicondyles in a plane perpendicular to the shaft axis. The NSA and AVA of the generic femur were calculated to be 123 and 17°, respectively.

To use the Torsion Tool for the femur, the participant's NSA and AVA are required as input. The NSA and AVA angles of the generic femur are subtracted from these input angles to attain the required rotation angles. Three subsequent transformations are then performed (Fig. 2A). First, vertices describing the femoral head, neck and greater trochanter are rotated. The NSA is adjusted by a rotation about the axis perpendicular to the neck and shaft axis, while AVA is achieved by a rotation about the shaft axis. Second, the vertices describing the lesser trochanter and proximal shaft are rotated by a linearly decreasing AVA as a function of superior-inferior distance along the femoral shaft axis. Third, the femoral head, neck, trochanters and shaft are translated to return the femoral head to its original position. The distal shaft is then gradually adjusted to fit to the femoral epicondyles, which did not move within the process. Since the positions of both the femoral head and epicondyles do not alter in the transformation process, the hip and knee joint centres are not affected. Finally, femoral muscle attachments are adjusted by applying the same transformations as for the femur bone geometry. Updated femur geometry and muscle attachments are added to a new subject-specific OpenSim model (Fig. 2B).

2.2. Evaluation of the tool for the femur

Fig. 3 provides an overview of how the Torsion Tool was evaluated, using MRI (slice thickness 1.1 mm, slice increments 1.1 mm, voxel size 0.83x0.83x1.0 mm) from a previously conducted study (Kainz et al., 2017), which included participants with a wide range of NSA and AVA. The femurs from six typically developing children (12.5 ± 3.6 years (mean \pm standard deviation), 149.2 ± 16.2 cm, 34.3 ± 20.3 kg) and 13 children with CP (10.5 ± 4.0 years, 133.5 ± 16.8 cm, 30.4 ± 11.3 kg) were segmented using Mimics v17 (Materialise, Leuven, Belgium). Data sets from typically developing children and the children with CP were combined, since sample sizes were too small to make a valid comparison between the groups and groups differed in characteristics (for subgroup result, see Appendix A). Target NSA and AVA from segmentations were calculated using methods described by Kainz et al. (2020). This resulted in a range for NSA from 119.7 to 145.8° (mean $133.1 \pm 6.2^\circ$), and for AVA from 4.3 to 46.9° (mean $21.5 \pm 8.9^\circ$). Angles were used in the Torsion Tool to create subject-specific OpenSim models with personalised femoral geometry. Both personalised and generic femurs were scaled uniformly using scaling factors derived from the OpenSim scaling tool for a static trial from each participant (Kainz et al., 2017). Scaled personalised and scaled generic femurs were then registered to MRI segmentations using n-point and global registration in 3-Matic (Materialise, Leuven, Belgium).

To evaluate the Torsion Tool performance, registered personalised and generic femurs were compared with the MRI segmentations. First, NSA and AVA were extracted from the personalised and generic femurs, and compared to measurements from MRI segmentations. Second, the agreement of the personalised and generic femurs with the segmented femur geometries was calculated using the following four error metrics: maximum, root mean square (RMS) and mean distances to quantify surface inaccuracies, and Jaccard index, which is a measure ranging from 0 to 1 to quantify volume similarity (Davico et al., 2019; Suwarganda et al., 2019). Differences in error metrics between the personalised and generic femurs were compared using paired-samples T-tests (version 20, SPSS INC., Chicago, IL, USA). Additionally, the relationship between error metrics and the magnitude of the NSA and AVA deviations was investigated using linear regressions.

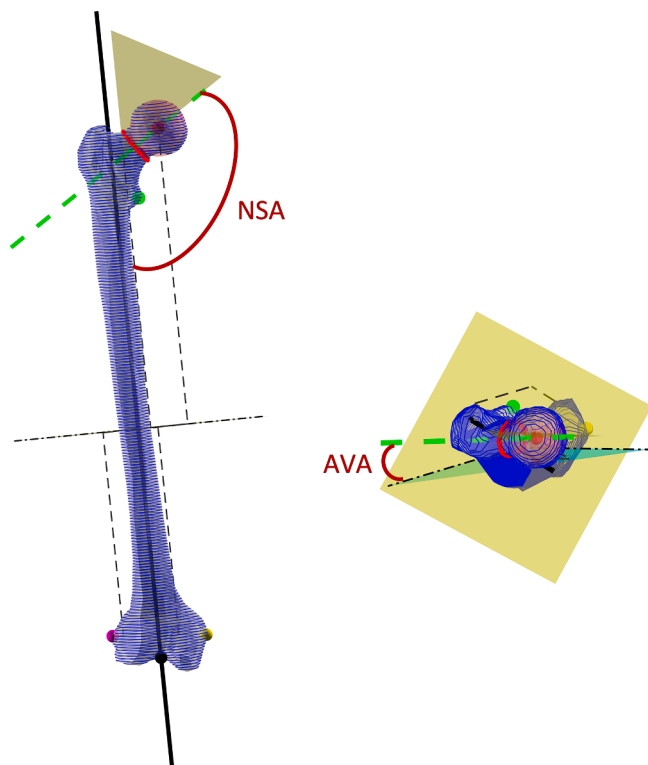


Fig. 1. The axes and planes used to calculate and personalise the NSA (left) and AVA (right). The dashed green line represents the neck axis, the black solid line the shaft axis. (For interpretation of the references to colour in this figure legend, the reader is referred to the web version of this article.)

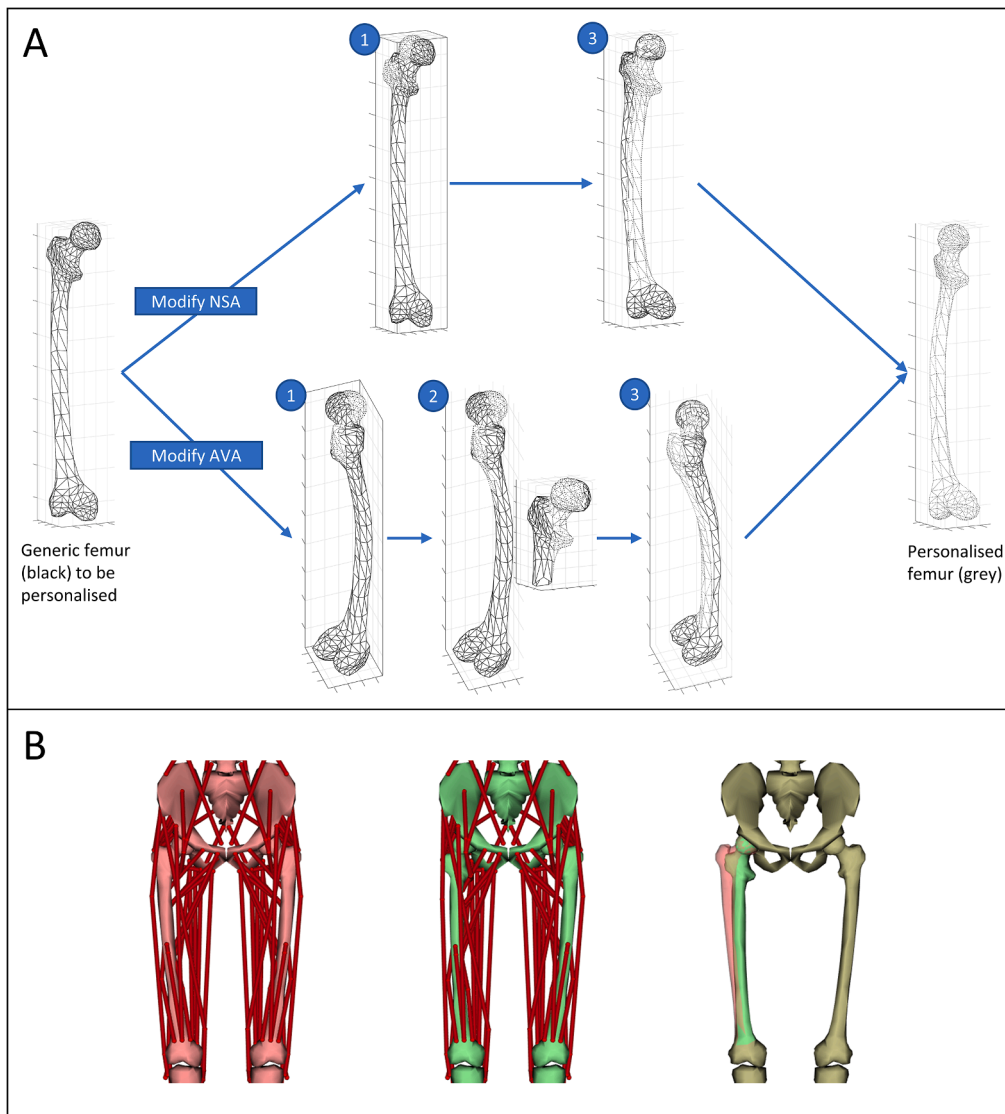


Fig. 2. (A) The three steps of increasing the NSA (top) and AVA (bottom) by 20° , with the black lines indicating the generic femur, and the grey dashed lines indicating the newly created personalised femur. Step 1: The femoral head, neck and greater trochanter are rotated by the NSA and AVA. Step 2: The lesser trochanter and proximal shaft are rotated by a linearly decreasing AVA as a function of superior-inferior distance along the femoral shaft axis. Step 3: The original position of the femoral head is restored by translating the femoral head, neck, trochanters and shaft. (B) The OpenSim model before (red) and after (green) this modification. (For interpretation of the references to colour in this figure legend, the reader is referred to the web version of this article.)

3. Results

Errors in NSA and AVA were significantly lower for the personalised femurs compared to the generic femurs ($p < 0.001$; Fig. 4A). The NSA differed $1.4 \pm 1.3^\circ$ and $10.1 \pm 5.8^\circ$ for the personalised and generic femurs respectively. Difference in AVA was $1.5 \pm 1.7^\circ$ for the personalised femurs, and $7.5 \pm 7.1^\circ$ for the generic femurs.

When comparing agreement between the personalised and generic femurs with the segmented femurs (Fig. 4B), the maximum distance was 19% lower for the personalised femur, the RMS distance was 18% lower, and the Jaccard index was 9% higher, which were all significant differences ($p < 0.001$).

The femurs with larger deviations in NSA and AVA resulted in a larger improvement with respect to NSA and AVA when using the tool, indicated by lower slopes for the linear regression for the personalised femurs compared to generic femurs (Fig. 5A). Further, femurs with higher deviations showed a higher improvement in error metrics when using the Torsion Tool, indicated by slopes significantly deviating from zero ($\beta < 0$ for the change in maximum and RMS distances; $\beta > 0$ for the change in Jaccard index; Fig. 5B).

4. Discussion

In this study we developed the Torsion Tool for automatically implementing subject-specific tibial and femoral torsions in a generic OpenSim model, and evaluated the tool for the femur. The resulting personalised femurs showed NSA and AVA significantly closer to the NSA and AVA of the segmented femurs than the scaled generic femurs, indicating the tool performs as designed. Also, the overall geometry agreement with the segmented femur improved significantly after using the Torsion Tool, underlying its contribution in personalising the femoral geometry. These improvements were most prominent for femurs with higher deviations in NSA and AVA compared to the generic values, suggesting that this personalisation is particularly important in participants with a large deviation in NSA and/or AVA from the generic model, e.g., children and patients with pathological femoral geometries.

Personalised femurs showed significantly lower errors in NSA and AVA. Although these errors were not zero, partially explained by the code calculating the angles that relies on random fitting, the error in NSA and AVA did not get worse for any subject, and overall shape agreement improved. Compared to a previous study looking at creating personalised paediatric bones (Davico et al., 2019), the Jaccard index between the linearly scaled and segmented femurs in our study was lower (0.48 in our study vs. 0.54 in Davico et al.). This may be due to the

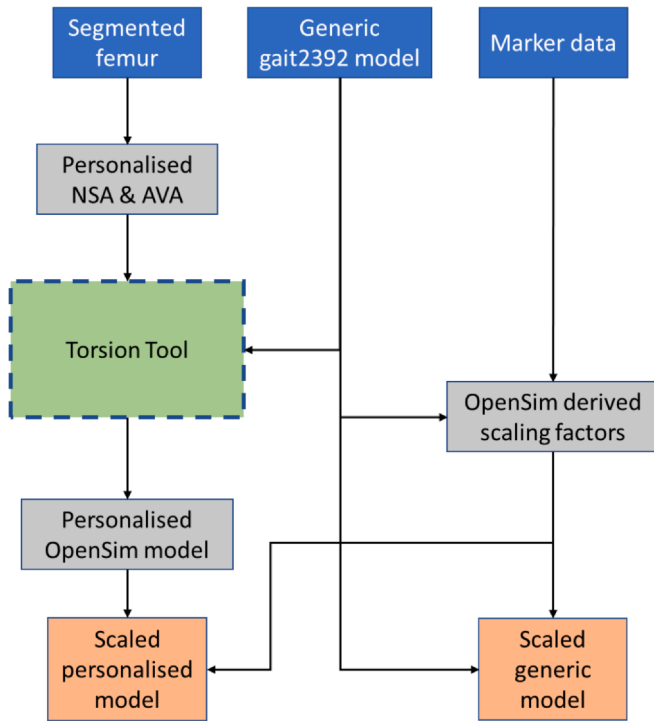


Fig. 3. Flowchart illustrating the steps undertaken to create the scaled personalised and generic model for each participant.

fact that our study cohort did not only contain typically developing children, but also children with CP. Improvements in the Jaccard index and RMS distance by using the Torsion Tool were not as large as when using statistical shape modelling and morphing techniques to create

subject-specific femoral geometries (Davico et al., 2019), but this may be expected since only a relatively small part of the femur was adjusted by the presented tool. Nevertheless, the NSA and AVA are likely the most important aspects of the femur because of their impact on muscle-tendon moment arms (see Appendix B for the impact of the tool on moment arms) and consequently muscle and joint contact forces (Arnold and Delp, 2001; Correa et al., 2011; Kainz et al., 2020).

The only input that the Torsion Tool requires are the participant’s torsion angles, which can be derived from (sparse) imaging methods, with computed tomography (CT) being considered the gold standard. For example, Sangeux et al. (2015) have described a protocol to obtain NSA and AVA from CT. Low-dose biplanar radiography methods, such as EOS (EOS imaging®, Paris, France), have also been shown to be accurate (Buck et al., 2012; Folinai et al., 2013; Thépaut et al., 2016), and may be preferred for their low radiation dose compared to CT. After adding the participant’s angles into the code, the tool runs within 30 seconds on a standard laptop (6 core Intel® Core™ i7-8750H @2.20 GHz., 8 GB RAM), adding only a minimal time burden to any musculoskeletal modelling pipeline. If individual NSA and AVA are not available, the tool could be used to create population-specific musculoskeletal models if population-specific NSA and AVA are known. This is not only relevant for pathological populations, but also for typically developing children, since it is known that NSA and AVA change during development (Fabry et al., 1994).

A limitation of the tool is that it is currently only implemented for a single model (Delp et al., 1990). However, this model is among the most commonly used models in literature, and, moreover, the code can be easily modified to be used with different generic models (e.g., Arnold et al., 2010; Rajagopal et al., 2016). Additionally, the tool also allows tibial torsion to be personalised, but this was not analysed in this study since no segmented tibia MRIs were available for our subjects. However, this part of the tool could also be useful for the community, and has therefore been included in the release. Another limitation is that mass and inertial properties were not adjusted by the tool, but their changes

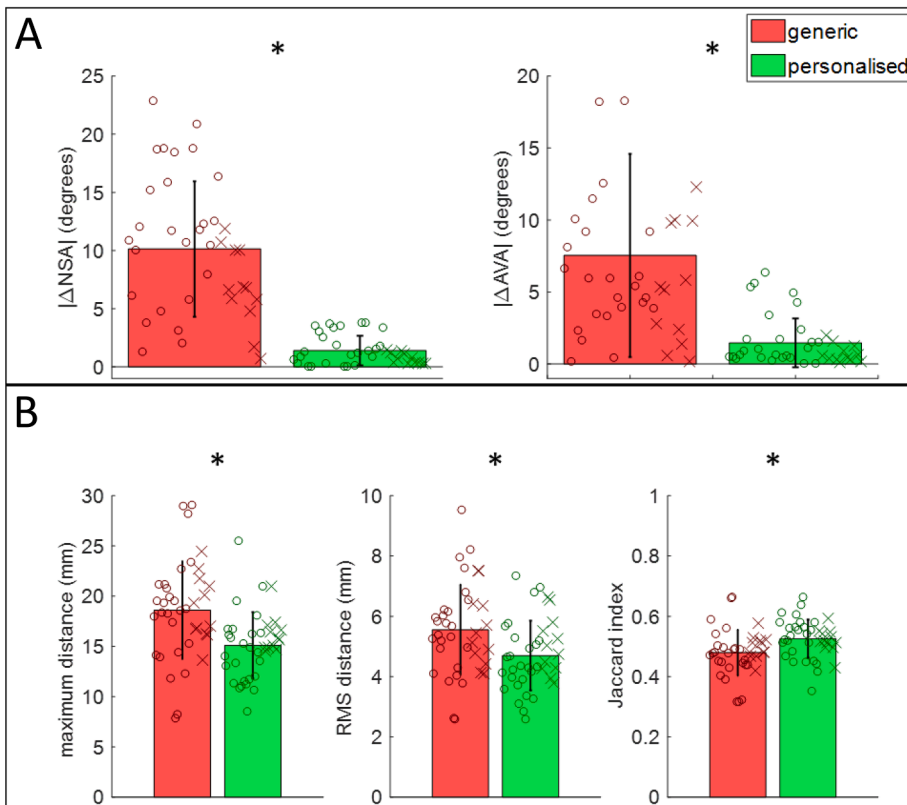


Fig. 4. The performance and effect of the tool. A: The absolute difference between the NSA and AVA of the segmented femurs and the scaled generic (red bars) and personalised femurs (green bars). B: Error metrics comparing the segmented femurs and the scaled generic (red bars) and personalised femurs (green bars). The error bars indicate the standard deviations. For the individual points, ‘o’ indicate participants with cerebral palsy and ‘x’ indicate typically developing participants. * indicate significant differences between generic and personalised femurs ($p < 0.001$). (For interpretation of the references to colour in this figure legend, the reader is referred to the web version of this article.)

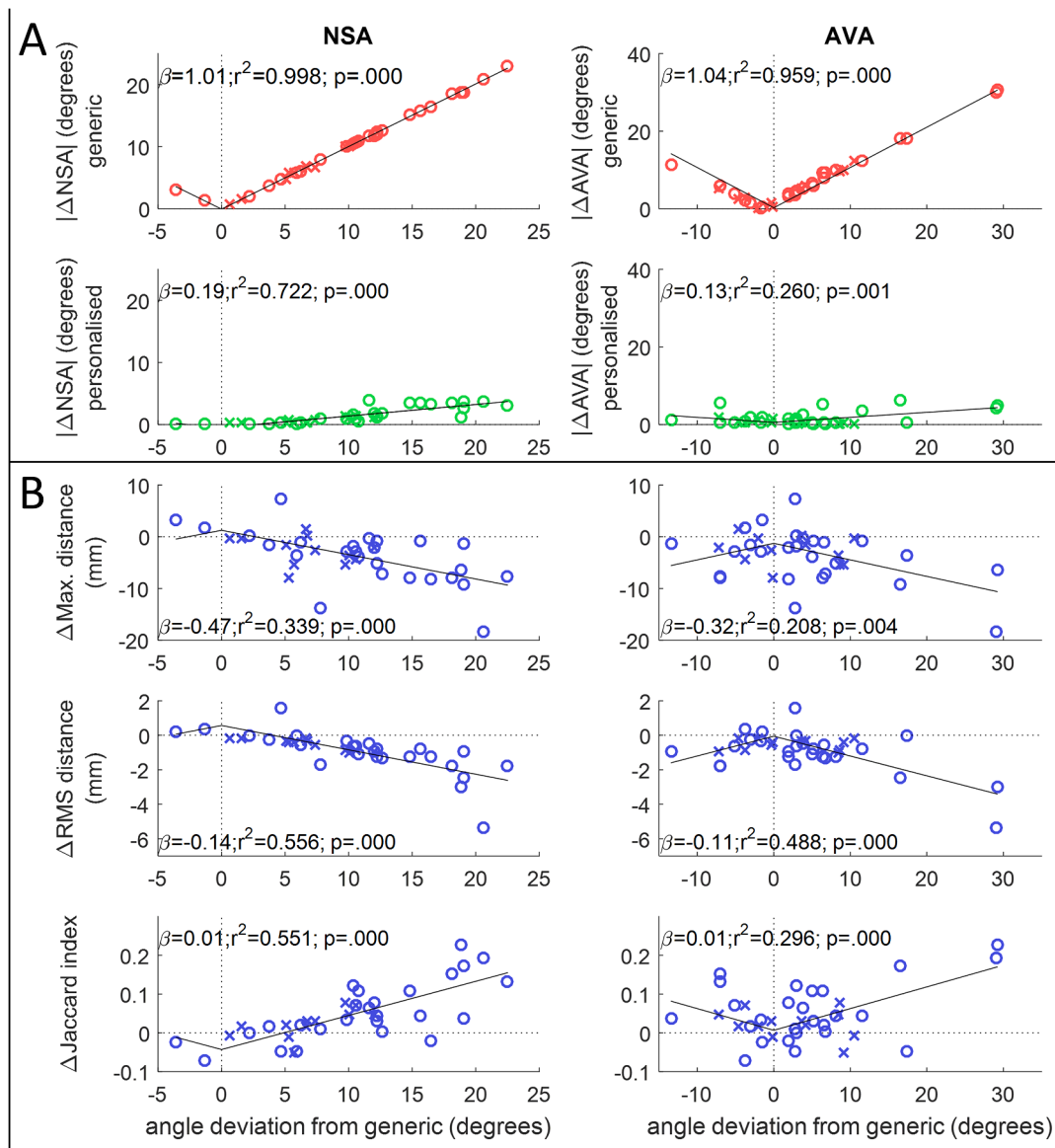


Fig. 5. The effect of the magnitude of NSA and AVA personalisation on (A) the error in the NSA and AVA compared to the segmented femur for the generic and personalised model and (B) on the change in error metrics when using the tool (personalised-generic). Deviations are shown for the full range of negative and positive deviations being used, regression analyses were performed for the absolute deviations since no different effects of positive and negative deviations were expected. β = slope of the linear regression. 'o' indicate participants with cerebral palsy and 'x' indicate typically developing participants.

are expected to be minimal since only a relatively small part of the femur is being rotated. A suggestion for further development of the tool would be the inclusion of personalising femoral neck length. Furthermore, the effects of including the personalised geometry on functional simulation outcomes such as musculotendon lengths and forces during gait, have not been evaluated yet. However, moment arms were shown to be affected by the tool (Appendix B) and several studies showed the impact of personalised NSA and AVA on these outcomes during gait (Arnold et al., 2001; Arnold and Delp, 2001; Correa et al., 2011; Scheys et al., 2008). Hence, it can be assumed that using the Torsion Tool would improve the accuracy of musculoskeletal simulations, especially for pathologies with large torsional deformities.

In conclusion, the Torsion Tool, available through <https://simtk.org/projects/torsiontool>, allows an automatic, fast and user-friendly way of personalising geometry in an OpenSim musculoskeletal model which directly can be used for movement simulations and analyses. The next step is to apply the tool in simulations and compare its performance to scaled generic and MRI-based models, to evaluate the effect of this

way of personalisation on functional and clinically-relevant outcomes.

Declaration of Competing Interest

The authors declare that they have no known competing financial interests or personal relationships that could have appeared to influence the work reported in this paper.

Acknowledgements

The authors would like to thank Lorenzo Pitto for providing the code to calculate the NSA and AVA angles. This study was supported by a Griffith University Advanced Queensland GCORE Postgraduate Research Scholarship to KV and by Amsterdam Movement Sciences, under the Innovation Call 2018, Tenure Development grant to MK.

Appendix A. Supplementary material

Supplementary data to this article can be found online at <https://doi.org/10.1016/j.jbiomech.2021.110589>.

References

- Arnold, A.S., Blemker, S.S., Delp, S.L., 2001. Evaluation of a Deformable Musculoskeletal Model for Estimating Muscle-Tendon Lengths During Crouch Gait. *Ann. Biomed. Eng.* 29, 263–274. <https://doi.org/10.1114/1.1355277>.
- Arnold, A.S., Delp, S.L., 2001. Rotational moment arms of the medial hamstrings and adductors vary with femoral geometry and limb position: Implications for the treatment of internally rotated gait. *J. Biomech.* 34, 437–447. [https://doi.org/10.1016/S0021-9290\(00\)00232-3](https://doi.org/10.1016/S0021-9290(00)00232-3).
- Arnold, E.M., Ward, S.R., Lieber, R.L., Delp, S.L., 2010. A model of the lower limb for analysis of human movement. *Ann. Biomed. Eng.* 38, 269–279. <https://doi.org/10.1007/s10439-009-9852-5>.
- Bobroff, E.D., Chambers, H.G., Sutherland, D.H., Sartoris, D.J., Wyatt, M.P., Sutherland, D.H., 1999. Femoral Anteversion and Neck-Shaft Angle in Children With Cerebral Palsy. *Clin. Orthop. Relat. Res.* 1–11.
- Buck, F.M., Guggenberger, R., Koch, P.P., Pfirmann, C.W.A., Fm, B., Guggenberger, R., Pp, K., 2012. Femoral and Tibial Torsion Measurements With 3D Models Based on Low-Dose Biplanar Radiographs in Comparison With Standard CT Measurements. *Musculoskelet. Imaging* 607–612. <https://doi.org/10.2214/AJR.11.8295>.
- Correa, T.A., Baker, R., Kerr Graham, H., Pandy, M.G., 2011. Accuracy of generic musculoskeletal models in predicting the functional roles of muscles in human gait. *J. Biomech.* 44, 2096–2105. <https://doi.org/10.1016/j.jbiomech.2011.05.023>.
- Davico, G., Pizzolato, C., Killen, B.A., Barzan, M., Suwarganda, E.K., Lloyd, D.G., 2010. 3D reconstruction of the lower extremity to study orthopaedic surgical procedures for musculoskeletal modelling. *Biomech. Model. Mechanobiol.* <https://doi.org/10.1007/s10237-019-01245-y>.
- Davico, G., Pizzolato, C., Lloyd, D.G., Obst, S.J., Walsh, H.P.J., Carty, C.P., Health, A., Centre, G., Gcore, R.E., Health, M., 2020. Increasing level of neuromusculoskeletal model personalisation to investigate joint contact forces in cerebral palsy: A twin case study. *Clin. Biomech.* 72, 141–149. <https://doi.org/10.1016/j.clinbiomech.2019.12.011>.
- Delp, S.L., Loan, J.P., Hoy, M.G., Zajac, F.E., Topp, E.L., Rosen, J.M., 1990. An interactive graphics-based model of the lower extremity to study orthopaedic surgical procedures. *IEEE Trans. Biomed. Eng.* 37, 757–767. <https://doi.org/10.1109/10.102791>.
- Fabry, G., Cheng, L.X., Molenaers, G., 1994. Normal and abnormal torsional development in children. *Clin. Orthop. Relat. Res.* 22–26 <https://doi.org/10.1097/00003086-199405000-00005>.
- Folainis, D., Thelen, P., Delin, C., Radier, C., Catonne, Y., Lazenec, J.Y., 2013. Measuring femoral and rotational alignment: EOS system versus computed tomography. *Orthop. Traumatol. Surg. Res.* 99, 509–516. <https://doi.org/10.1016/j.otsr.2012.12.023>.
- Fox, A.S., Carty, C.P., Modenese, L., Barber, L.A., Lichtwark, G.A., 2018. Simulating the effect of muscle weakness and contracture on neuromuscular control of normal gait in children. *Gait Posture* 61, 169–175. <https://doi.org/10.1016/j.gaitpost.2018.01.010>.
- Hicks, J., Arnold, A., Anderson, F., Schwartz, M., Delp, S., 2007. The effect of excessive tibial torsion on the capacity of muscles to extend the hip and knee during single-limb stance. *Gait Posture* 26, 546–552. <https://doi.org/10.1016/j.gaitpost.2006.12.003>.
- Kainz, H., Hoang, H., Pitto, L., Wesseling, M., Van Rossom, S., Van Campenhout, A., Molenaers, G., De Groote, F., Desloovere, K., Jonkers, I., 2019. Selective dorsal rhizotomy improves muscle forces during walking in children with spastic cerebral palsy. *Clin. Biomech. (Bristol, Avon)* 65, 26–33. <https://doi.org/10.1016/j.clinbiomech.2019.03.014>.
- Kainz, H., Hoang, H.X., Stockton, C., Boyd, R.R., Lloyd, D.G., Carty, C.P., 2017. Accuracy and reliability of marker-based approaches to scale the pelvis, thigh, and shank segments in musculoskeletal models. *J. Appl. Biomech.* 33, 354–360. <https://doi.org/10.1123/jab.2016-0282>.
- Kainz, H., Killen, B.A., Wesseling, M., Perez-Boerema, F., Pitto, L., Aznar, J.M.G., Shefelbine, S., Jonkers, I., 2020. A multi-scale modelling framework combining musculoskeletal rigid-body simulations with adaptive finite element analyses, to evaluate the impact of femoral geometry on hip joint contact forces and femoral bone growth. *PLoS One* 15, 1–18. <https://doi.org/10.1371/journal.pone.0235966>.
- Kainz, H., Modenese, L., Lloyd, D.G., Maine, S., Walsh, H.P.J., Carty, C.P., 2016. Joint kinematic calculation based on clinical direct kinematic versus inverse kinematic gait models. *J. Biomech.* 49, 1658–1669. <https://doi.org/10.1016/j.jbiomech.2016.03.052>.
- Killen, B.A., Luz, S.B., Lloyd, D.G., Zhang, A.D.C.J., Saxby, T.F.B.D.J., 2020. Automated creation and tuning of personalised muscle paths for OpenSim musculoskeletal models of the knee joint. *Biomech. Model. Mechanobiol.* <https://doi.org/10.1007/s10237-020-01398-1>.
- Lundy, D.W., Ganey, T.M., Ogden, J.A., Guidera, K.J., 1998. *J. Pediatr. Orthop.* 18, 528–534.
- Modenese, L., Montefiori, E., Wang, A., Wesarg, S., Viceconti, M., Mazzà, C., 2018. Investigation of the dependence of joint contact forces on musculotendon parameters using a codified workflow for image-based modelling. *J. Biomech.* 73, 108–118. <https://doi.org/10.1016/j.jbiomech.2018.03.039>.
- Rajagopal, A., Dembia, C.L., DeMers, M.S., Delp, D.D., Hicks, J.L., Delp, S.L., 2016. Full-Body Musculoskeletal Model for Muscle-Driven Simulation of Human Gait. *IEEE Trans. Biomed. Eng.* 63, 2068–2079. <https://doi.org/10.1109/TBME.2016.2586891>.
- Robin, J., Graham, H.K., Selber, P., Dobson, F., Smith, K., Baker, R., 2008. Proximal femoral geometry in cerebral palsy. *J. Bone Joint Surg. Br.* 90B, 1372–1379. <https://doi.org/10.1302/0301-620X.90B10.20733>.
- Sangeux, M., Pascoe, J., Graham, H.K., Ramanauskas, F., Cain, T., 2015. Three-Dimensional Measurement of Femoral Neck Anteversion and Neck Shaft Angle. *J. Comput. Assisted Tomogr.* 39 (1), 83–85. <https://doi.org/10.1097/RCT.0000000000000161>.
- Scheys, L., Van Campenhout, A., Spaepen, A., Suetens, P., Jonkers, I., 2008. Personalized MR-based musculoskeletal models compared to rescaled generic models in the presence of increased femoral anteversion: Effect on hip moment arm lengths. *Gait Posture* 28, 358–365. <https://doi.org/10.1016/J.GAITPOST.2008.05.002>.
- Steele, K.M., DeMers, M.S., Schwartz, M.H., Delp, S.L., 2012. Compressive tibiofemoral force during crouch gait. *Gait Posture* 35, 556–560. <https://doi.org/10.1016/j.gaitpost.2011.11.023>.
- Suwarganda, E.K., Diamond, L.E., Saxby, D.J., Lloyd, D.G., Bryce, A.K., Savage, T.N., 2019. Minimal medical imaging can accurately reconstruct geometric bone models for musculoskeletal models. *Plos* 14, e0205628. <https://doi.org/10.1101/432310>.
- Thépaud, M., Brochard, S., Leboucher, J., 2016. Measuring physiological and pathological femoral anteversion using a biplanar low-dose X-ray system: validity, reliability, and discriminative ability in cerebral palsy 243–250. <https://doi.org/10.1007/s00256-015-2298-y>.
- Valente, G., Crimi, G., Vanella, N., Schileo, E., Taddei, F., 2017. nmsBuilder: Freeware to create subject-specific musculoskeletal models for OpenSim. *Comput. Methods Programs Biomed.* 152, 85–92. <https://doi.org/10.1016/j.cmpb.2017.09.012>.
- van der Krogt, M.M., Delp, S.L., Schwartz, M.H., 2012. How robust is human gait to muscle weakness? *Gait Posture* 36, 113–119. <https://doi.org/10.1016/j.gaitpost.2012.01.017>.
- Veerkamp, K., Schallig, W., Harlaar, J., Pizzolato, C., Carty, C.P., Lloyd, D.G., van der Krogt, M.M., 2019. The effects of electromyography-assisted modelling in estimating musculotendon forces during gait in children with cerebral palsy. *J. Biomech.* <https://doi.org/10.1016/J.JBIOMECH.2019.05.026>.
- Wesseling, M., De Groote, F., Meyer, C., Corten, K., Simon, J.P., Desloovere, K., Jonkers, I., 2016. Subject-specific musculoskeletal modelling in patients before and after total hip arthroplasty*. *Comput. Methods Biomech. Biomed. Engin.* 19, 1683–1691. <https://doi.org/10.1080/10255842.2016.1181174>.